The influence of degree-of-branching and molecular mass on the interaction between dextran and Concanavalin A in hydrogel preparations intended for insulin release

Ian Benzeval[+], Adrian Bowyer[*], John Hubble[+]
([+] Department of Chemical Engineering, [*] Department of Mechanical Engineering, University of Bath, Bath BA2 7AY)

Keywords: Dextran, hydrogel, branching, insulin, concanavalin

Abstract

The interactions of a number of commercially available dextran preparations with the lectin concanavalin A (ConA) have been investigated. Dextrans over the molecular mass range $6x10^3$ - $2x10^6$ g mol^{-1} were initially characterised in terms of their branching, and hence terminal ligand density, using NMR. This showed a range of branching ratios between 3 and 5%, but no clear correlation with molecular mass.

The bio-specific interaction of these materials with ConA was investigated using microcalorimetry. The data obtained was interpreted using a number of possible binding models reflecting the known structure of both dextran and the lectin.

The results of this analysis suggest that the interaction is most appropriately described in terms of a two-site model. This offers the best compromise for the observed relationship between data and model predictions and the number of parameters used based on the chi squared values obtained from a nonlinear least-squares fitting procedure. A two-site model is also supported by analysis of the respective sizes of the dextrans and the ConA tetramer.

Using this model the relationship between association constants, binding energy and molecular mass was determined.

1. Introduction

Hydrogels offer the possibility of releasing drugs or hormones into the body in response to metabolic demands or circadian rhythms. For many drug treatments this, as opposed to the less responsive release from injection or ingestion of drugs, would be superior. In particular, the treatment of type I diabetes in this manner would reduce occurrences of hypo- and hyperglycaemia.

Dextran and concanavalin A have been used to produce glucose-responsive hydrogels for the treatment of type I diabetes [1, 2]. This facile method has been shown to create hydrogels which can respond to glucose under physiological conditions without producing potentially harmful by-products. The published work only focused on one dextran size, though commercially available dextran is available in a range of molecular mass fractions. Lectins, such as ConA, are known to bind based on more than just an interaction with the terminal group of a polysaccharide chain, the other monomers within the chain also interact with the lectin. Therefore there are several properties of the dextran molecule that can influence the binding: the size of the

molecule and the branching ratio will affect how many lectins can be contacted simultaneously whilst the length of the branches will affect the manner and strength of the bond with the lectin, all of which are likely to have a profound influence upon the ability of the hydrogel to crosslink effectively. A knowledge of the differing strengths of the affinity bond between the lectin and the various different dextran sizes available would enable the composition of the hydrogel to be tailored to the desired response rate.

Dextran molecules are produced as exopolysaccharides by various strains of bacteria and are primarily reported as having branching ratios of 5% [3-5]. However, research by Kim *et al.* has been performed to show that an uncontrolled batch fermentation will result in a variable degree of branching [6]. Knowledge of the number of branches (and therefore of the number of terminal glucose groups) is essential if an accurate ligand density is to be used when measuring the binding association and enthalpy of the dextran-ConA interaction. Therefore in this study dextran branching was measured by NMR using the observation that the non-hydroxyl hydrogens within a glucose unit, and thus within a dextran molecule, have different spin energies depending upon their position. This allows the structure of the dextran molecules to be evaluated [7-12]. Specifically, the hydrogen bound to the anomeric carbon has differentiable peaks dependent upon the carbon of the neighbouring glucose to which it is attached.

The strength of the affinity interaction was measured using isothermal titration calorimetry (ITC). This technique, whilst providing data on the strength of the affinity interaction, cannot provide information on the kinetics. However, compared to surface plasmon resonance and other techniques capable of measuring kinetics, ITC requires neither the dextran nor the lectin to be immobilised. The resulting data therefore gives a better representation of how the two components will behave in a hydrogel.

The physical size of the dextran molecules is also a consideration when investigating this type of system. Though the ConA tetramer has four possible saccharide affinity interaction sites, it is conceivable that not all of these will be simultaneously available owing to spatial restrictions within the hydrogel.

2. Materials and Methods

2.1 Materials

The dextrans (6, 11, 17, 43, 64, 500 and 2000 kD), D-glucose, maltose, maltotriose, concanavalin A, TRIS (TRIZMA base), NaN_3, $MnCl_2.4H_2O$, Na_2HPO_4 and D_2O were all purchased from Sigma Aldrich, Poole, UK. $MgCl_2.6H_2O$, $CaCl_2.2H_2O$, NaCl, NaOH and HCl were purchased from Fisher Scientific, Loughborough, UK.

All experiments, with the exception of the NMR, were performed in the following buffer solution: 20mM TRIS, 150mM sodium chloride, 0.5mM calcium chloride, magnesium chloride and manganese chloride, and 0.02 wt% sodium azide corrected to pH 7.4 using hydrochloric acid and sodium hydroxide.

2.2 Methods

2.2.1 Branch density calculation through NMR.

The calculation of the branching rate was performed using ^{1}H NMR. The experiments were performed using a 400 MHz Bruker NMR spectrometer, (Bruker, Coventry, UK). The experiments were based on the ability to differentiate between the peaks of the hydrogen on the anomeric carbon [7-12]. The difference in environment of this hydrogen is caused by the location of a covalent bond between the glucose monomers (Figure 1).

At room temperature, C_1 hydrogen absorption was found to overlap with the hydroxyl group hydrogens and the hydrogen impurities in the solvent (due to incomplete deuteration). Scans were therefore taken at $55^{o}C$, as this causes a shift in the spectra due to the additional energy of the nuclei. Here this resulted in the C_1 hydrogen absorption being shifted downfield (to a greater ppm) of the hydroxyl peak - facilitating subsequent analysis.

2.2.2 Binding analysis using microcalorimetry

ITC experiments were performed using a MicroCal Isothermal Titration Calorimeter, (MicroCal, GE Healthcare Ltd. Bucks. UK). Each run comprised 31 injections of 5 μl each at 2 minute intervals. Syringe rotation was set to 400 r.p.m. and the reference power set to 10 μcal s^{-1}[13,14].

All experiments with the ITC were performed in the previously detailed buffer at pH 7.4 and at $37^{o}C$. This meant the experiments were conducted at physiological pH and temperature. The solutions were found to be more stable, particularly the ConA solution, if they were frozen after being made and thawed prior to use each day. The concentration of tetrameric ConA in the cell was kept at 0.1mM, this being the highest usable concentration that avoided adverse viscosity effects. The dextrans were used at as high a concentration as possible, again to minimise viscosity effects. The dextrans used were of 6, 11, 17, 43, 64, 500 and 2000kD molecular mass.

To correct for thermal changes due to dilution effects, background runs were performed. This involved injecting the same dextran solutions as used in the standard tests into buffer devoid of ConA. This showed the energy signature of the dilution effects of the buffer, which could then be subtracted from the standard run to give the energy signature which was solely due to the binding interactions.

The data obtained from the ITC was fitted to several mechanistic models based on the possibility of each of the four monomers of a ConA tetramer forming affinity links with dextran. The quality of the fit was measured by calculating the chi squared value of the data. A simple calculation of the total error was not appropriate owing to the additional degrees of freedom introduced by the greater number of variables present in the multi-site binding equations (Equation 1) [15-17].

$$
\begin{aligned}
K_1 &= \frac{4}{1} KI_1 = \frac{[MX]}{[M][X]} \\
K_2 &= \frac{3}{2} KI_2 = \frac{[MXX]}{[MX][X]} \\
K_3 &= \frac{2}{3} KI_3 = \frac{[MXXX]}{[MXX][X]} \\
K_4 &= \frac{1}{4} KI_4 = \frac{[MXXXX]}{[MXXX][X]}
\end{aligned}
\qquad (1)
$$

$$
\chi^2 = \frac{\sum (Model - data)^2}{(n_p - p)} \qquad (2)
$$

Where K_n is the association constant, KI_n the intrinsic association constant, *[M]* the concentration of ConA, *[X]* the concentration of dextran and *[MX]*, *[MXX]*, *[MXXX]* and *[MXXXX]* the concentrations of the ConA-dextran complexes. n_p is the number of data points and p the number of parameters.

The line of best fit in Figure 4A, for a single site interaction (Langmuir form), shows systematic deviation from the data, as confirmed in the residual plot, Figure 4C. In Figure 4B, where a two-site sequential binding model was used, the corresponding residual plot, Figure 4D, shows a more random residual distribution.

The validity of the binding models was assessed on the basis of the χ^2 values. This is a summation of the square of the error between the model and the data, divided by the number of degrees of freedom (Equation 2). The number of degrees of freedom is found by subtracting the number of parameters from the number of data points to identify the statistical quality of the model. Further analysis of the data using models accounting for all possible interactions from one to four sites considering the possibility of both independent (non-sequential) and sequential interactions showed that a two-site sequential model provided the best fit to the data. This can be seen by the higher chi-squared values of the other models in Table 2.

Each of the dextran sizes, D-glucose, maltose and maltotriose were run in duplicate and the data modelled using the data-fitting package Scientist v2 ® (Micromath, St. Louis, USA). The two-site binding model was used to obtain estimates of the binding parameters. The modelling for D-glucose, maltose and maltotriose was performed using the monomeric concentration of ConA as there were no size constraints associated with these small molecules.

3 Results

3.1 NMR

The ratio of the magnitudes of the NMR response peaks can be used to calculate the branching ratio, with the C_2 to C_6 hydrogens absorbing between 3.5 and 4.5 ppm and

C_1 hydrogens absorbing between 4.8 and 6.0 ppm. The spectra shown in Figure 2 and Figure 3 do not show the hydrogens of the hydroxyl groups. These peaks are not visible beneath the solvent-impurity peak between 4.5 and 4.8 ppm (there will still be a small amount of hydrogen present in the deuterated solvent). The total area of the C_2 to C_6 hydrogen peaks compared to the C_1 peaks should be 6:1. The ratio of the main chain α(1-6) groups to the branch α(1-3) will equal the branching ratio.

Comparison of the dextran spectrum to maltotriose in Figure 3 enables identification of the type of branches in the dextran. The maltotriose spectrum has three peaks in the C_1 region. The doublets A and C (4.9 and 5.5 ppm respectively) correspond to the α and β configurations of the reducing end C_1 [7-12]. The third peak, E (between 5.6 and 5.7 ppm) must therefore be due to the two α(1-4) linkages in maltotriose. This is confirmed by the ratio of areas of peaks E : A+C being 2:1. For the dextran spectrum (in bold) peaks A and C are the same as those of maltotriose. Peaks B and D must therefore correspond to the linkages of the main chain and of the branches respectively. The main-chain linkages are known to be α(1-6) in dextran, whilst the branches can either be α(1-3) or α(1-4), depending on the species used for production [11,18]. The triplet, D, does not appear at the same ppm as the maltotriose peak, E. Therefore, given that the maltotriose peak is known to be α(1-4), the dextran branches from this species must be α(1-3). The ratio of peak D to peak B gives the branching ratio of the dextran. These values for the branching ratio of the dextran preparations used are shown in Table 1.

Using these branching ratios the thermodynamics of the affinity interaction with ConA can be determined using isothermal titration calorimetry.

3.2 Isothermal Titration Calorimetry

The fitted binding parameters for each data set are shown in Table 3. The association constant of the primary binding site (Figure 5) has a general correlation of increasing binding strength with increasing molecular mass. The amount of energy released by these complexes does not follow a similar correlation, Figure 6. The data for the secondary binding site (Table 3) shows greater variation, both between replicates and between molecular masses. The energy released by the secondary binding sites ranges from ~10% for 11 kD dextran to ~40% for the 6 and 43 kD dextrans. The lower this figure, the harder it is for the fitting process to accurately predict the values. The greater strength of association for maltose, compared to D-glucose, is consistent with the accepted view of how lectins bind to saccharides, but this does not appear to hold for maltotriose.

Mangold et al. [19] have performed similar tests on monomeric and dimeric ConA using ITC. Titrations of various dendrimers with terminal mannose groups have shown that the association constant of binding increases as the number of terminal groups increases. However, the modelling performed in their work did not include sequential binding for the dimeric ConA.

The crystallographic work performed by Reeke *et al.* produced an image of the structure of ConA (Figure 7) [20]. The size of each monomer is approximately 4x4x4

nm [20]. Figure 7 shows that a ConA tetramer exists as two planes of substrate binding sites. Units I and II have approximately 5nm between their binding sites with III and IV in a similar position on the opposite face of the tetramer. The hydrodynamic radius of dextran has been shown to be between 1.5 and 30nm for dextrans up to 2000 kD [21, 22]. It is therefore unlikely that more than two dextran molecules can bind to a ConA tetramer simultaneously because of physical constraints. This is supported by the sequential site analysis which showed the three- and four-site models to be inappropriate, and by the D-glucose, maltose and maltotriose data that allowed full tetrameric binding (Table 3). The weak strength of the secondary bond compared to the primary can also be explained by the size restrictions; the presence of a dextran bound to one side of the ConA tetramer will limit the angle from which a second dextran can approach and thus bind.

4. Conclusion

The analysis of the branching ratio of the dextrans by NMR has shown that the branching ratio is not the 5% quoted in most references and also not predictable by molecular mass. Therefore, for any quantitative work to be performed, the branching ratio of each batch of dextran used must be determined prior to analysis.

The interaction between ConA and dextran has been thermodynamically investigated. It has been shown that a weak prediction of the primary association constant can be made from the size of the dextran molecule. No prediction of the enthalpic change of binding is possible. Lectin binding sites are shallow compared to those of enzymes and antibodies [23], with binding being enhanced by secondary effects of the molecule “lying” across the surface of the protein, reflecting the biological role of oligosaccharide recognition. As the length of the dextran chain increases the amount of additional binding should increase, making the binding stronger. The reason for this pattern not being more strongly confirmed by the ITC data is that the length of the branches was not known.

There is a suggestion that the secondary binding is weaker than the primary binding, implying negative cooperativity. This is likely to be due to physical constraints, similar to those that prevent tertiary and quaternary binding, rather than changes in chemical conformation. It is therefore possible to state that, should this work be continued to test non-toxic proteins with dextran, the number of monomers bound together is not the important factor - the relative position and distance between the saccharide binding sites is the essential characteristic.

Acknowledgements
IB gratefully acknowledges the financial support of an EPSRC studentship.

References

[1] R. Zhang, M. Tang, A. Bowyer, R. Eisenthal, J. Hubble, Synthesis and Characterization of a D-glucose Sensitive Hydrogel Based on CM-dextran and Concanavalin A, React. Funct. Polym. 66 (2006) 757-767.
[2] M. Tang, R. Zhang, A. Bowyer, R. Eisenthal, J. Hubble, A Reversible Hydrogel Membrane for Controlling the Delivery of Macromolecules., Biotechnol. Bioeng. 8 (2002) 47-53.
[3] A. Jeanes, W.C. Haynes, C.A. Wilham, J.C. Rankin, E.H. Melvin, M.J. Austin, J.E. Cluskey, B.E. Fisher, H.M. Tsuchiya, C.E. Rist, Characterization And Classification Of Dextrans From Ninety-Six Strains Of Bacteria, J. Am. Chem. Soc.76 (1954) 5041-5052.
[4] A. Jeanes, C.A. Wilham, Periodate Oxidation Of Dextran, J. Am. Chem. Soc. 72 (1950) 2655-2657.
[5] Sigma-Aldrich data sheet – accessed 02/11/2009 http://www.sigmaaldrich.com/etc/medialib/docs/Sigma-Aldrich/Product_Information_Sheet/d5251pis.Par.0001.File.tmp/d5251pis.pdf
[6] D. Kim, J.F. Robyt, S.-Y. Lee, J.-H. Lee, Y.-M. Kim, Dextran Molecular Size And Degree Of Branching As A Function Of Sucrose Concentration, pH And Temperature Of Reaction Of Leuconostoc Mesenteroides B-512FMCM Dextransucrase, Carbohydr. Res. 338 (2003) 1183-1189.
[7] D. Williams, I. Fleming, Spectroscopic Methods in Organic Chemistry, sixth ed., McGraw-Hill Higher Education, Maidenhead, 2008.
[8] W.M. Pasika, L.H. Cragg, The Detection and Estimation of Branching in Dextran by Proton Magnetic Resonance Spectroscopy, Can. J. Chem. 41 (1962) 293-299.
[9] F.R. Seymour, R.D. Knapp, S.H. Bishop, Correlation of the Structure of Dextrans to their 1H-NMR Spectra, Carbohydr. Res. 74 (1979) 77-92.
[10] V.B. Sokolov, K.A. Krasnov, I. Matyushichev, Yu, B.V. Passet, 1H NMR Study of Distribution of Functional Groups in Carboxymethyl Dextran, Zhurnal Prikl. Him. 72 (1999) 701-703.
[11] N.W.H. Cheetham, E. Fiala-Beer, Dextran Structural Details from High-Field Proton NMR Spectroscopy. Carbohydr. Polym. 14 (1991) 149-158.
[12] N.H. Maina, M. Tenkanen, H. Maaheimo, R. Juvonen, L. Virrki, NMR Spectroscopic Analysis of Exopolysaccharides Produced by Leuconostoc citreum and Weissella confuse, Carbohydr. Res. 343 (2008) 1446-1455.
[13] MicroCal, L., VP-ITC MicroCalorimeter User's Manual, Northampton, MA: MicroCal.
[14] T. Wiseman, S. Williston, J.F.Brandts, L.-N. Lin, Rapid Measurement of Binding Constants and Heats of Binding Using a New Titration Calorimeter. Anal. Biochem. 179 (1989) 131-137.
[15] A. Cornish-Bowden, Fundamentals of Enzyme Kinetics, first ed., Butterworths, Southampton, 1979.
[16] J.M. Baldwin, A Model Of Co-Operative Oxygen Binding To Haemoglobin, Br. Med. Bull. 32 (1976) 213-218.
[17] D. Michel, Co-operative Equilibrium Curves Generated By Ordered Ligand Binding To Multi-Site Molecules, Biophys. Chem. 129 (2007) 284-288.
[18] D. Voet, J.G. Voet, Sugars and Polysaccharides, in Biochemistry, second ed., Wiley, New York City, 1995.

[19] S.L. Mangold, M.J. Cloninger, Binding of Monomeric and Dimeric Concanavalin A to Mannose-Functionalized Dendrimers, Org. Biomol. Chem. 4 (2006) 2458-2465.
[20] G.N. Reeke, J.W. Becker, G.M. Edelman, The Covalent and Three-Dimensional Structure of Concanavalin A: IV. Atomic Coordinates, Hydrogen Bonding and Quaternary Structure, J. Biol. Chem. 250 (1975) 1525-1547.
[21] C.E. Ioan, T. Aberle, W. Burchard, Structure Properties of Dextran. 2. Dilute Solution. Macromolecules 33 (2000) 5730-5739.
[22] W.M. Saltzman, Drug Delivery: Engineering Principles for Drug Therapy, first ed. Oxford University Press, New York, 2001.
[23] S. Elgavish, B. Shaanan, Lectin-Carbohydrate Interactions: Different Folds, Common Recognition Principles, Trends Biochem. Sci. 22 (1997) 462-467.

Captions

Figure 1 (a) Structure of α-D-glucose molecule. (b) Dextran chain of α(1-6) bonds (main chain, i) with a free anomeric end (ii) and an α(1-3) bond (branch, iii)

Figure 2 ^{1}H spectra for 17kD Dalton dextran. The peaks between 3.5 and 4.5ppm correspond to the C_2 to C_6 hydrogen atoms. The peak at 4.75ppm is the hydroxyl and solvent impurity peak. Peaks from 4.8 to 5.8ppm correspond to the C_1 hydrogen atoms and these are enlarged in Figure 3 for clarity.

Figure 3 ^{1}H spectra for 17kD Dalton dextran (bold) and maltotriose.

Figure 4 Titration of ConA with dextran. Plots A and B both represent 31 5μl injections of 11kD dextran into 0.1mM ConA. The line of best fit in plot A shows a Langmuir type binding, plot B shows a sequential sites model. Plots C and D are the residual errors (C applies to A, D applies to B) (1μCal = 4.184μJ).

Figure 5 Intrinsic association constants for primary binding of D-glucose, maltose (a glucose dimer), maltotriose (a glucose trimer) and various dextrans with ConA.
The data is the mean of two replicates; error bars are +/- one standard deviation. Dextran data modelled using tetrameric ConA concentration. Non-dextran data modelled using monomeric concentration of ConA.

Figure 6 Enthalpy change of primary binding of D-glucose, maltose, maltotriose and various dextrans with ConA.

Figure 7 Structure of a ConA tetramer [20]. It consists of two pairs of dimers on top of each other. Ca, Mn and S represent the calcium ion, manganese ion and substrate binding sites respectively. Each sub-unit is approximately 4x4x4 nm.

Table 1 Branching ratio by dextran molecular mass.

Table 2 Comparison of data analysis models based on size of error.

Table 3 ITC Binding parameters.

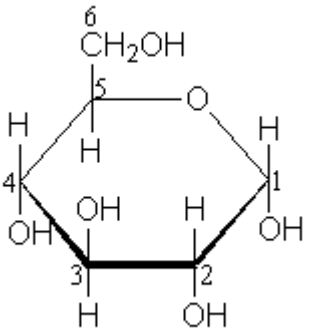

(a)

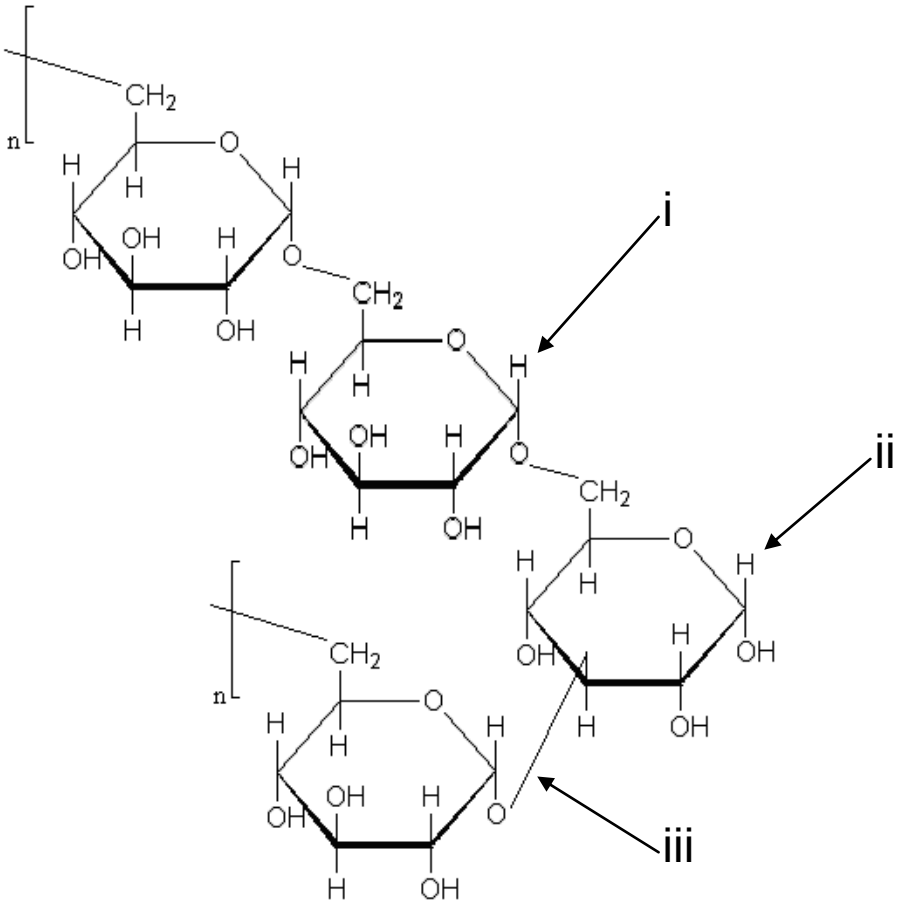

(b)

Figure 1

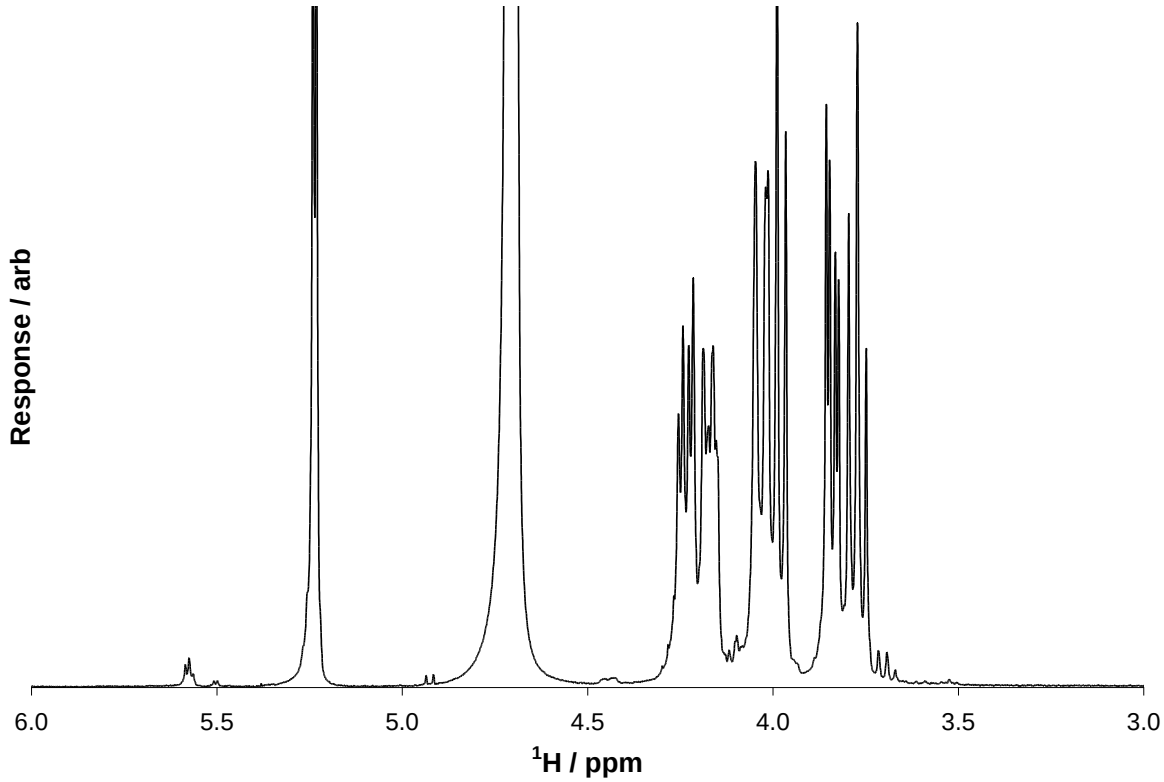

Figure 2

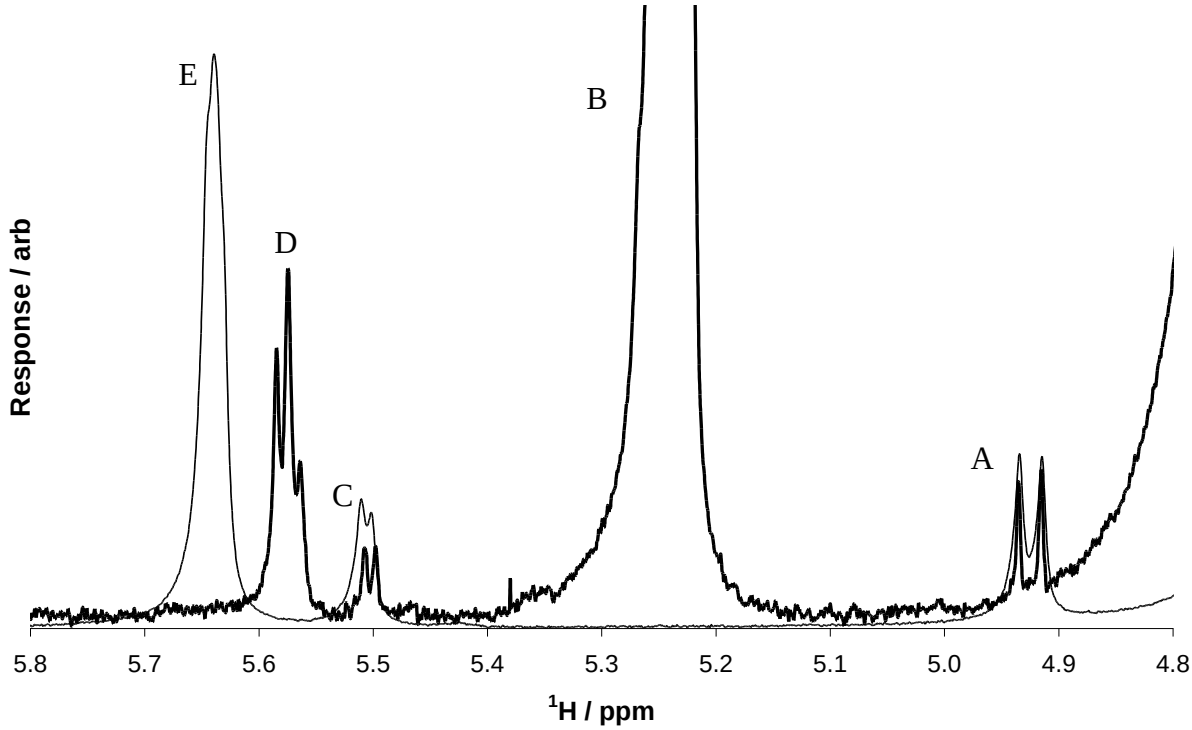

Figure 3

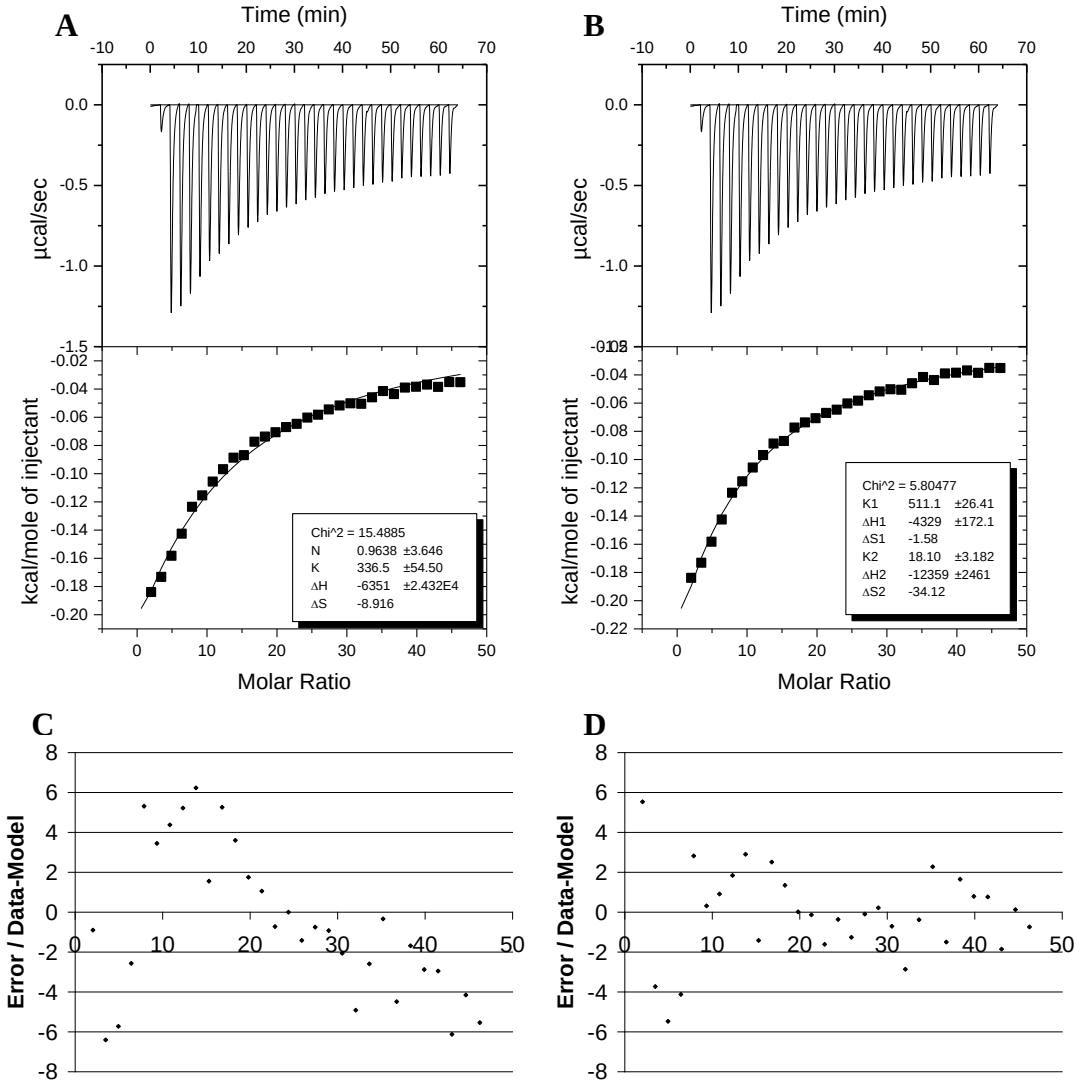
A
Time (min)
µcal/sec
kcal/mole of injectant
Molar Ratio
Chi^2 = 15.4885
N 0.9638 ±3.646
K 336.5 ±54.50
ΔH -6351 ±2.432E4
ΔS -8.916
B
Time (min)
µcal/sec
kcal/mole of injectant
Molar Ratio
Chi^2 = 5.80477
K1 511.1 ±26.41
ΔH1 -4329 ±172.1
ΔS1 -1.58
K2 18.10 ±3.182
ΔH2 -12359 ±2461
ΔS2 -34.12
C
Error / Data-Model
D
Error / Data-Model

Figure 4

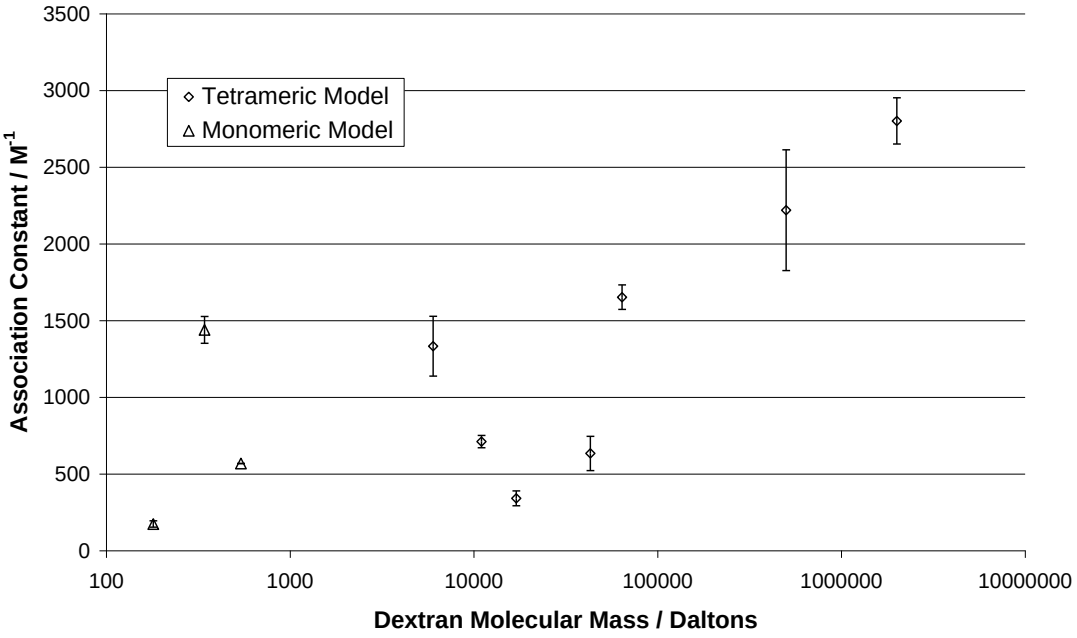
3500
3000
2500
2000
1500
1000
500
0
Tetrameric Model
Monomeric Model
Association Constant / M-1
100
1000
10000
100000
1000000
10000000
Dextran Molecular Mass / Daltons

Figure 5

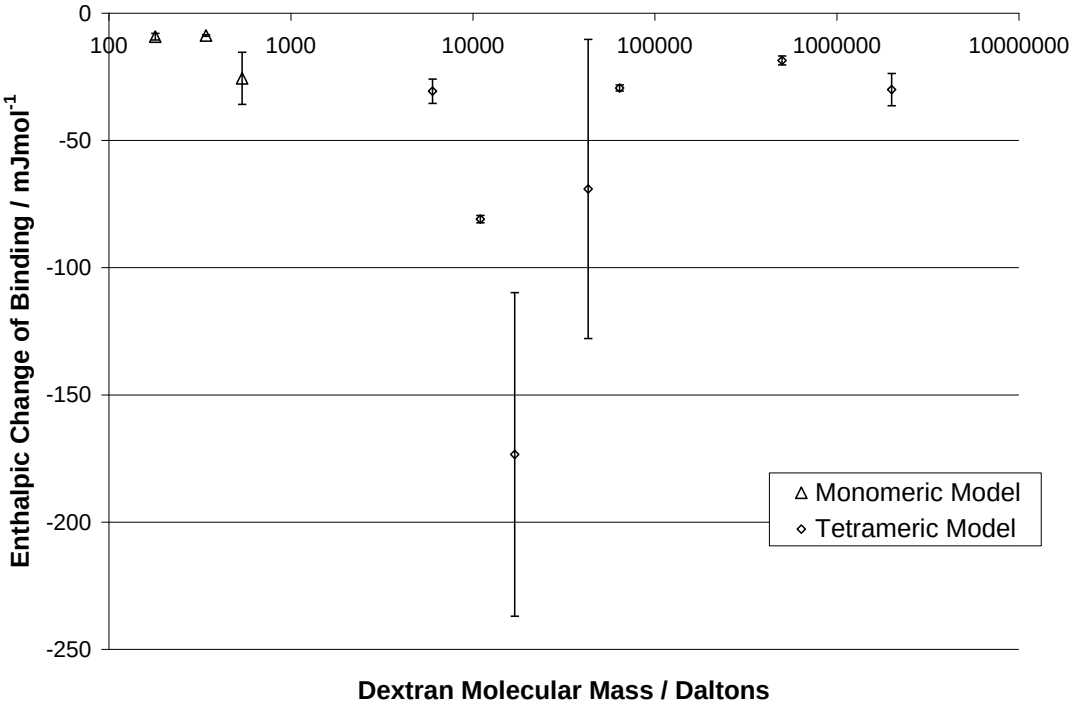
0
-50
-100
-150
-200
-250
100
1000
10000
100000
1000000
10000000
Enthalpic Change of Binding / mJmol-1
Dextran Molecular Mass / Daltons
Monomeric Model
Tetrameric Model

Figure 6

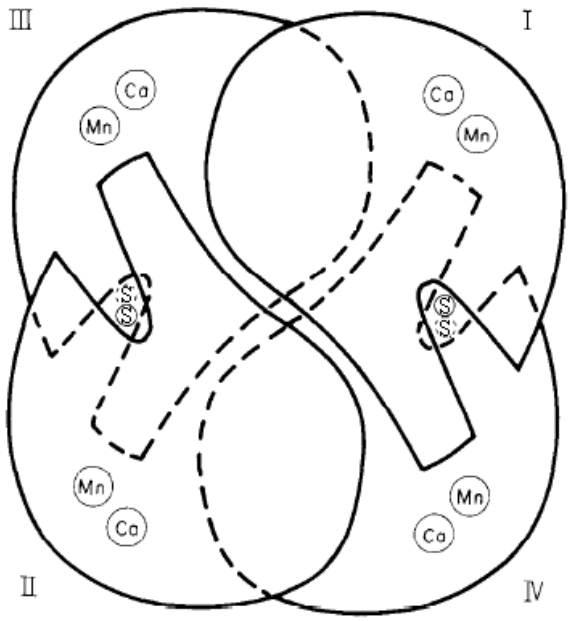

Figure 7

RMM of Dextran	Branching ratio / %
6000	5.5
11000	3.0
17000	3.9
43000	3.9
64000	4.8
500000	4.6
2000000	4.1

Table 1

		K_a, ΔH equal			K_a, ΔH different		
ConA Units	1	2	3	4	2	3	4
Number of parameters	2	2	2	2	4	6	8
χ^2	3.200	3.400	3.619	5.421	0.491	0.609	0.615

Table 2

Dextran MW / kD	K_{a1} / M^{-1}	ΔH_1 / $kJmol^{-1}$	K_{a2} / M^{-1}	ΔH_2 / $kJmol^{-1}$	Second site energy release / %
Glucose – rep1	159	-10.2	-	-	-
Glucose – rep2	189	-8.31	-	-	-
Maltose – rep1	1380	-8.60	-	-	-
Maltose – rep2	1500	-9.02	-	-	-
Maltotriose – rep1	568	-18.4	-	-	-
Maltotriose – rep2	569	-32.9	-	-	-
6 – rep1	1190	-34.1	109	-155	38.2
6 – rep2	1470	-27.3	225	-73.1	44.8
11 – rep1	683	-82.0	14.5	-1320	9.9
11 – rep2	740	-79.9	35.1	-427	7.7
17 – rep1	376	-128	2.07	-17700	15.1
17 – rep2	307	-218	1.02	-29000	8.2
43 – rep1	714	-27.5	200	-106	49.0
43 – rep2	556	-111	125	-417	31.1
64 – rep1	1710	-28.6	676	-53.3	37.3
64 – rep2	1600	-30.2	6.93	-2160	16.0
500 – rep1	2500	-19.8	132	-93.4	30.8
500 – rep2	1940	-17.3	198	-51.1	31.7
2000 – rep1	2700	-25.6	6.15	-333	2.1
2000 – rep2	2910	-34.5	0.35	-54100	12.5

Table 3